Supporting Information

Partial substitution induced centrosymmetric to noncentrosymmetric structure transformation and promising second-order nonlinear optical properties of $(K_{0.38}Ba_{0.81})Ga_2Se_4$

Ya-Nan Li, Yang Chi, Zong-Dong Sun, Huaiguo Xue, Nian-Tzu Suen and Sheng-Ping Guo*

School of Chemistry and Chemical Engineering, Yangzhou University, Yangzhou, Jiangsu 225002, P. R. China

Corresponding author: spguo@yzu.edu.cn

Experimental Section

Synthesis. All starting materials were used as received without further purification. Single crystals of **1** were synthesized by a high temperature solid state reaction. The starting materials were Ga (99.9 %), Se (99.9 %), Ba (99.9 %), and KI as flux. The total mass of Ba, Ga, and Se was 500 mg, and 400 mg KI (99 %) additional. The molar ratios of Ba : Ga : Se were 1 : 2 : 4. The mixture was ground into fine powder in an agate mortar and further pressed into a pellet, followed by being loaded into a quartz tube. The quartz tube was evacuated to be 1×10^{-4} torr and flame-sealed. The tube was placed into a muffle furnace, heated from room temperature to 1223 K with the speed of 30 K/h, and several intermediate equilibrated temperatures were set to homogenize the reactive system and prevent quartz tube's broken. The heat preservation at 1223 K was maintained for 5 days, finally cooled down to 573 K at a speed of 5 K per hour and powered off. The green crystals of **1** were

obtained, which were then washed with alcohol and pure water, followed by being ultrasounded.

Structure Refinement and Crystal Data. Single crystals of **1** was picked out under a microscope and then measured on a Bruker D8 QUEST diffractometer with graphite-monochromated Mo-$K\alpha$ radiation (λ = 0.71073 Å) at 296 K for data collection. The Direct Method and the SHELXTL program package were used to solve and refine the crystal structure.[1] The solution result indicates that K and Ba co-occupy the Ba site with the molar ratio of 2.13, and their total site occupation factor is 0.593, which is consistent with the result of an energy dispersive X-ray spectroscope (EDS, Bruker, Quantax) (Fig. S1 and Table S1). All the atoms' anisotropic displacement parameters and a secondary extinction correction were included in the final refinement. The detailed crystallographic tables are listed in Table S2. Tables S3 and S4 demonstrate the atomic coordinates, equivalent isotropic displacement parameters, and selected bond lengths, respectively.

Power X-ray Diffraction (PXRD) Characterization. The purity was confirmed by PXRD analysis. The PXRD pattern was collected with a Bruker D8 Advance diffractometer at 40 kV and 100 mA for Cu-$K\alpha$ radiation (λ = 1.5406 Å) with a scan speed of 5 °/min at room temperature. The simulated pattern was produced using the Mercury v2.1 program provided by the Cambridge Crystallographic Data Center and single-crystal reflection data. The PXRD pattern corresponds well with the simulated one, indicating a pure sample. (Fig. S2).

Infrared (IR) and UV-Vis-NIR Diffuse Reflectance Spectra. The IR spectrum was measured using a TENSOR27 FT-IR spectrophotometer in the range of 400–4000 cm^{-1}. The powdery sample was pressed into a pellet with KBr. The diffuse reflectance spectrum was

recorded with a computer-controlled Varian Cary 5000 UV-Vis-NIR spectrometer in the wavelength range of 200–1700 nm. A $BaSO_4$ plate was used as a reference, on which the finely ground powdery sample was coated. The absorption spectrum was calculated from reflection spectrum by the Kubelka-Munk function.[2]

SHG and powder LIDT measurements: SHG measurement on powder crystalline sample of **1** was evaluated by a modified Kurtz-NLO system using a 2.1 μm Q-switch laser radiation.[3] Polycrystalline powdery sample of **1** was ground and sieved into particle size ranges of (5–25, 25–45, 45–75, 75–100, 100–150, and 150–210 μm). Benchmark AGS with the similar particle sizes were served as the standard at 2.1 μm. Each sample was loaded into a glass microscope cover slide, surrounded by a 1 mm thick silicone insole with a 5 mm diameter hole. Then they were put into little-tight boxes and a pulsed IR beam from a Q-switched laser with a wavelength of 2.1 μm radiated the samples. The SHG signals were collected by the detector and showed the peaks on the oscilloscope.

The single-pulse measurement method was used to evaluate the LIDT value of **1**. The crystalline sample with the particle size range (75~100 μm) was selected and pressed into a glass microscope covered slide. The sample was radiated by 1064 nm laser with a pulse width τ_p of 10 ns in a 1 Hz repetition. The laser facula area is 0.152053 cm^2. The measurement was performed under an optical microscope once single-pulse radiation was passed, and the laser power increased until the damaged spot was observed. Then, the laser power was marked, and the area of the damaged spot was measured as the damage threshold parameters of the sample. The laser beam power was monitored by a Nova II sensor display with a PE50-DIT-C energy sensor. The damaged spot was measured using a Vernier caliper.

Theoretical calculation: Because there is co-occupation of K and Ba in **1**，a 1 × 1 × 5 supercell based on the imaginary $K_{0.4}Ba_{0.8}Ga_2Se_4$ was constructed along the characteristic *z* axis of the crystal system for calculation. Based on density functional theory (DFT), the band structure, density of states (DOS), and optical properties were calculated by using CASTEP code in Materials Studio.[4] The Perdew-Burke-Ernzerhof (PBE) of Generalized Gradient Approximation (GGA) was selected as the functional, and the ultrasoft pseudopotential was chosen.[5] The plane-wave cutoff energy of 330 eV and the threshold of 5×10^{-7} eV were also set for the self-consistent-field convergence of total electronic energy. The calculation of the Brillouin Zone was performed using 3 × 3 × 1 Monkhorst-Pack *k*-point meshes. The Fermi level (E_f = 0 eV) was selected for reference. The orbital electrons were treated as valence electrons, K-$3s^2 3p^6 4s^1$, Ba-$5s^2 5p^6 6s^2$, Ga-$3d^{10} 4s^2 4p^1$, and Se-$4s^2 4p^4$. The dielectric function $\varepsilon(\omega) = \varepsilon_1(\omega) + i\varepsilon_2(\omega)$, in which $\varepsilon_1(\omega)$ and $\varepsilon_2(\omega)$ were respectively defined as the real and imaginary parts of dielectric function, was used to calculate and describe the optical properties. Linear and second-order nonlinear optical properties were described in the dielectric function $\varepsilon(\omega) = \varepsilon_1(\omega) + i\varepsilon_2(\omega)$. The first order nonresonant susceptibility in the low-frequency region can be obtained from:

$$\chi_{ii}^{(1)}(\omega) = [\varepsilon_{ii}(\omega) - 1]/4\pi$$

The second-order susceptibilities can be expressed as follows using the first order linear polarization coefficient:[6]

$$\chi_{ijk}^{(2)}(\omega_3,\omega_1,\omega_2) = \frac{ma}{N^2 e^3}\chi_{ii}^{(1)}(\omega_3)\,\chi_{jj}^{(1)}(\omega_1)\chi_{kk}^{(1)}(\omega_2)$$

This formula is derived from the classical anharmonic oscillator models, *m*, *e*, and *N* are electron mass, electron charge, and atomic number density, respectively. It should be noted that the *N* here, for the crystal, should be the number of unit cells in the crystal. For all

condensed matter, N is close to 10^{22} cm^{-3}, and the nonlinear characteristic parameter a can be obtained from the experiment or theoretically.

For completeness, the NLO coefficients and Δn of AGS were also calculated using the same method.

Table S1. The Ba/K molar ratios in **1** from EDS results.

Single crystal of **1**	a	b	c
Ba/K molar ratio	14.27/7.32 = 1.95	12.84/6.67 = 1.92	13.03/5.63 = 2.31

Table S2. Crystal data and structure refinement parameters for **1**.

chemical formula	$K_{0.38}Ba_{0.81}Ga_2Se_4$ (**1**)
Fw	581.38
T (K)	296.15
Crystal system	tetragonal
Space group	*I*4*cm*
Z	2
a (Å)	8.0211(4)
b (Å)	8.0211(4)
c (Å)	6.2888(8)
V /Å^3	404.61(7)
D_{calc}g/cm^3	4.772
μ /mm^{-1}	28.598
F(000)	501.0
Radiation	Mo-$K\alpha$ (λ = 0.71073)
2θ range(°)	7.184 to 50.886
Measd. reflns	198
Reflections collected	860
Indep. reflns/R_{int}	203/0.0544
GOF on F^2	1.188
R1, wR2 ($I > 2\sigma(I)$)[a]	R1 = 0.0379, wR2 = 0.0943

R1, wR2 (all data)[a]	R1 = 0.0380, wR2 = 0.0944
$\Delta\rho$max/$\Delta\rho$min, e/Å^3	1.81/-1.29

[a]$R1 = ||F_o| - |F_c||/|F_o|$. [b]$wR2 = [w(F_o^2 - F_c^2)^2]/[w(F_o^2)^2]^{1/2}$.

Table S2. Atomic coordinates (× 10^4) and equivalent isotropic displacement parameters (U_{eq}[a], Å^2 × 10^3) for **1**.

Atom	Wyck. site	*x*	*y*	*z*	U_{eq}/Å^2
Ba(1)	4*a*	0	0	1330(50)	29.4(13)
K(1)	4*a*	0	0	1330(50)	29.4(13)
Ga(1)	4*b*	5000	0	1320(20)	8.8(9)
Se(1)	8*c*	3376.2(7)	1623.8(7)	3810.8(2)	10.3(8)

[a]U_{eq} is defined as one third of the trace of the orthogonalized U_{ij} tensor.

Table S3. Important bond lengths (Å) for **1**.

Bond	Dist./Å
Ba(1)–Se(1)#3	3.385(13)
Ba(1)–Se(1)#4	3.397(14)
Ba(1)–Se(1)#1	3.386(13)
Ga(1)–Se(1)#13	2.427(10)
Ga(1)–Se(1)#14	2.417(10)
Se(1)–K(1)#15	3.397(14)

Se(1)–K(1)#10	3.386(13)

Symmetry transformations used to generate equivalent atoms: #1 +*x*, -*y*, 1/2+*z*; #3 -*y*, +*x*, +*z*; #4 -1/2+*y*, 1/2-*x*, -1/2+*z*; #10 1/2+*x*, 1/2-*y*, +*z*; #13 1/2+*y*, 1/2-*x*, -1/2+*z*; #14 1-*x*, -*y*, +*z*; #15 1/2+*x*, 1/2+*y*, 1/2+*z*.

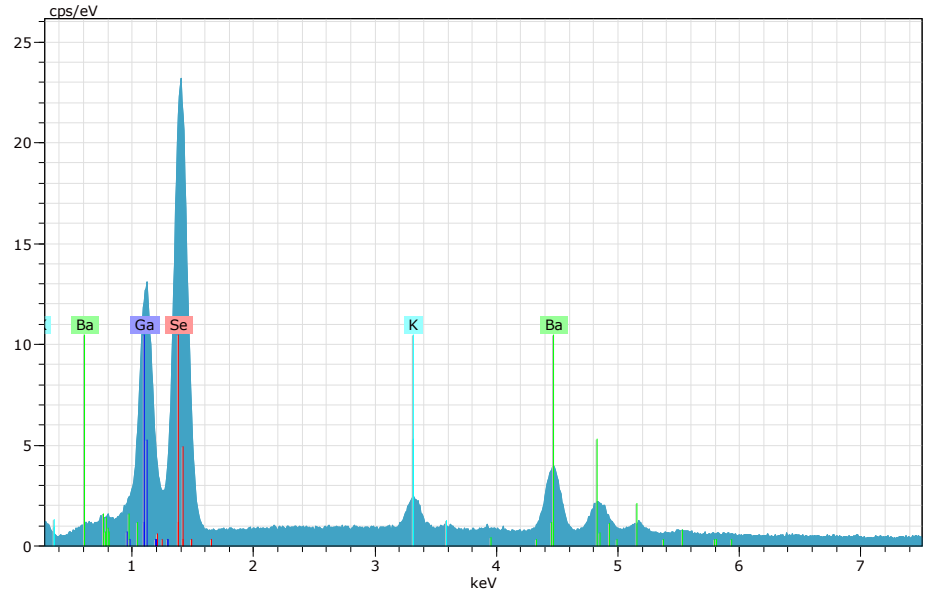

Fig. S1 EDS graph of single crystal of **1**.

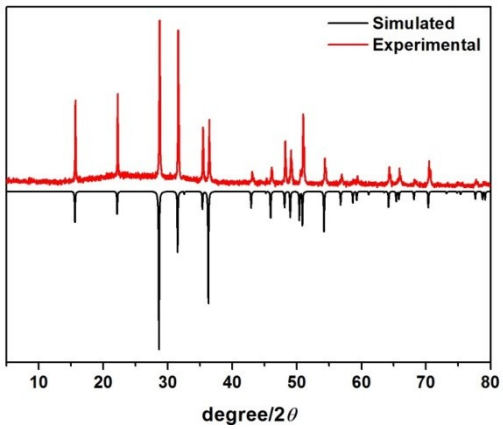

Fig. S2 Powder X-ray diffraction pattern of **1**.

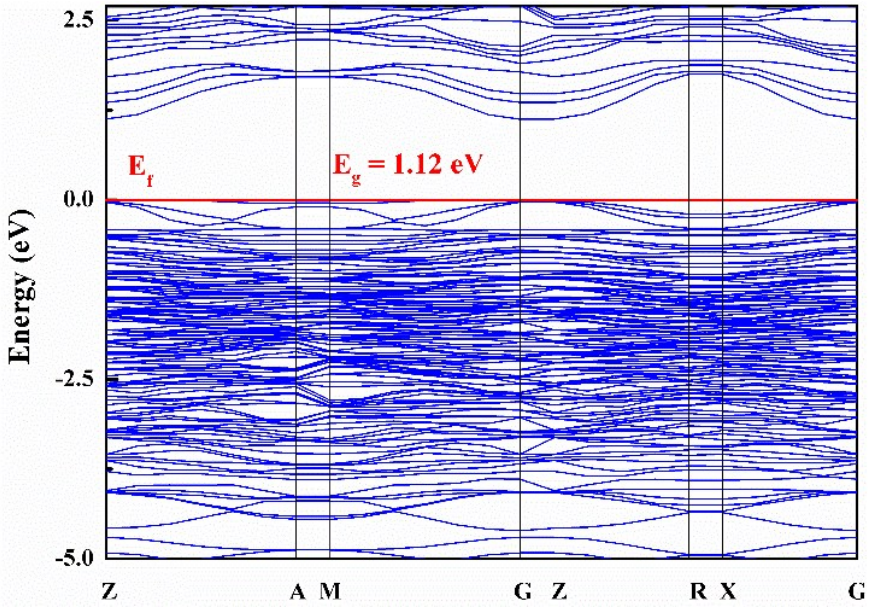

Fig. S3 Calculated band structure of **1**. The Fermi level is chosen as the energy 0 eV.

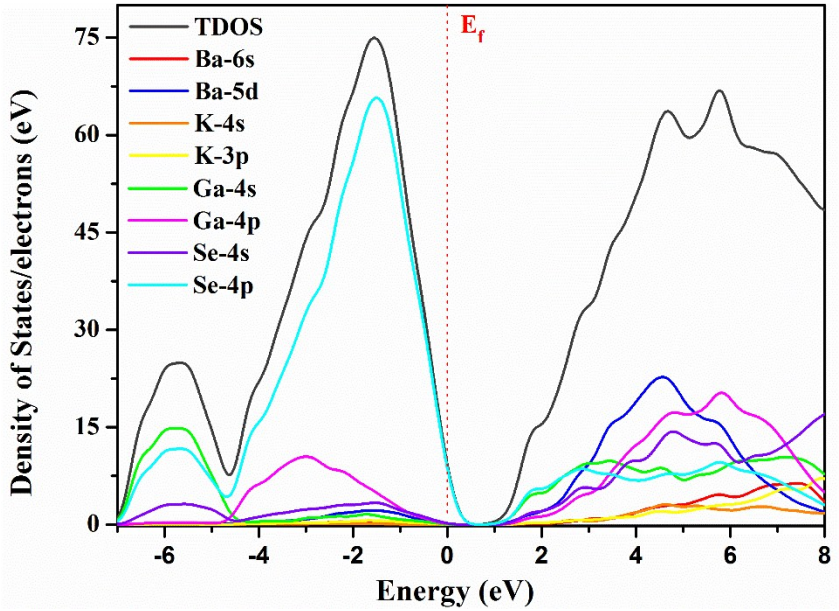

Fig. S4 Calculated DOS of **1**. The Fermi level is chosen as the energy 0 eV.

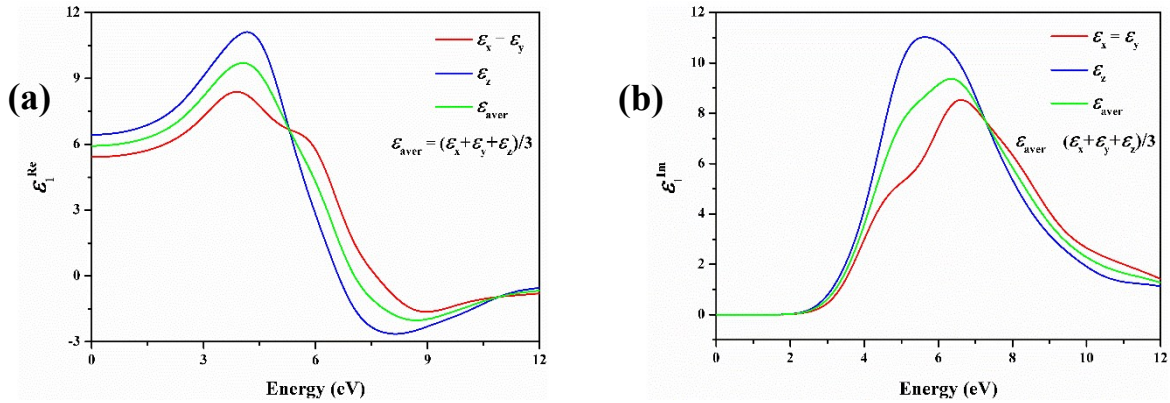

Fig. S5 The theoretical real (a) and imaginary (b) parts of the optical dielectric functions of **1**.

References

(1) O. V. Dolomanov, L. J. Bourhis, R. J. Gildea, J. A. K. Howard and H. Puschmann, *J. Appl. Crystallogr*., 2009, **42**, 339.

(2) (a) W. W. Wendlandt and H. G. Hecht, *Reflectance Spectroscopy.,* Interscience Publishers, New York, 1966; (b) G. Kortüm, *Reflectance Spectroscopy*, Springer., 1969.

(3) S. K. Kurtz and T. T. Perry, *J. Appl. Phys*., 1968, **39**, 3798-3813.

(4) (a) M. D. Segall, P. L. D. Lindan, M. J. Probert, C. J. Pickard, P. J. Hasnip, S. J. Clark and M. C. Payne, *J. Phys.: Condens. Matter.,* 2002, **14**, 2717; (b) V. Milman, B. Winkler, J. A. White, C. J. Pickard, M. C. Payne, E. V. Akhmatskaya and R. H. Nobes, *Int. J. Quantum Chem.,* 2000, **77**, 895-910.

(5) (a) D. R. Hamann, M. Schluter and C. Chiang, *Phys. Rev. Lett.,* 1979, **43**, 1494; (b) J. S. Lin, A. Qteish, M. C. Payne and V. Heine, *Phys. Rev., B* 1993, **47**, 4174.

(6) (a) S. N. Rashkeev, W. R. Lambrecht and B. Segall, *Phys. Rev. B.,* 1998, **57**, 3905; (b) C. Aversa and J. E. Sipe, *Phys. Rev. B.,* 1995, **52**, 14636-14645.